Journal of Biotechnology 306 (2019) 89–96

Contents lists available at ScienceDirect

Journal of Biotechnology

journal homepage: www.elsevier.com/locate/jbiotec

Mono-PEGylates of exenatide in branched and dimeric structures can improve *in vivo* stability and hypoglycemic bioactivity

Ngoc-Thanh Thi Nguyen[a], Sujin Jung[a,1], Seung Hwan Lee[a,*], Ok Nam Bae[a,2], E.K. Lee[b,*]

[a] Dept. of Bionanotechnology, Graduate School, South Korea
[b] College of Pharmacy, Hanyang University – ERICA, Ansan, 15588, South Korea

ARTICLE INFO

Keywords:
Exenatideanalogs
Mono-PEGylation
Homodimer PEGylate
Long-acting peptides
Hypoglycemic efficacy
Half-life

ABSTRACT

Exenatide, a synthetic version of exendin-4, is a glucagon-like peptide-1 receptor agonist (GLP-1RA) used for treating diabetes, but its relatively short half-life is a major disadvantage. In this study, we attempted residue-specific mono-PEGylation to the middle of the amino acid backbone to extend its *in vivo* half-life. Exenatide was point-mutated from Lys to Cys at the 12th residue to yield a variant (K12C), and PEG-maleimide of varying molecular weights (MW) (5, 10, 20, 40 kD) was site-specifically conjugated to yield a mono-PEGylate with branched T-shape molecular structure. In another approach, we conjugated a bis-maleimide PEG (10 kD) to the middle of two K12Cs to yield an H-shape homodimer PEGylate *In vitro* bioactivity assays indicated that: (1) PEGylates conjugated with higher MW PEG lead to stronger receptor binding, (2) the branched form was superior to the linear configuration in the binding, and (3) both T-shape and H-shape mono-PEGylates demonstrated better potency than the native exenatide, evidenced by lower EC_{50}. Db/db mouse experiments to evaluate *in vivo* hypoglycemic activity indicated that: (1) all mono-PEGylates resulted in improved glucose tolerance compared to the native exenatide, (2) the homodimer PEGylate demonstrated much stronger hypoglycemic activity, especially during the initial period, and (3) the H-shape and T-shape mono-PEGylates (40 kD) maintained hypoglycemia for up to *ca.* 168 and 140 h, representing approximately 12- and 14-fold increase, respectively, compared with the native exenatide. Our findings suggest that the exenatide mono-PEGylates in unclassical molecular structures can improve *in vivo* pharmacokinetics properties.

1. Introduction

Exenatide (Ex) is a 39-amino acid peptide of glucagon-like peptide-1 (GLP-1) receptor agonist with dipeptidyl peptidase IV (DPP-IV) resistant properties for an extended in-serum half-life *ca.* 2.4 h, which is significantly longer than that of GLP-1 (*ca.* 2–3 min) (Lund et al., 2014; Trujillo and Nuffer, 2014a; Edwards et al., 2001; Egan et al., 2002). Due to 53% amino acid homology with GLP-1, exenatide maintains similar biological functions which include increasing glucose-dependent insulin secretion, inhibiting high glucose secretion, decreasing the gastric empty rate, reducing food intake to promote body weight loss, and increasing the amount of β-cells (Gentilella et al., 2009). Exenatide was approved by the US FDA in 2005 as a Type II diabetes treatment. Numerous efforts have been made to further improve the pharmacokinetic properties of GLP-1 or its analogs through genetic and chemical modifications, *e.g.*, genetic fusion of human serum albumin (HSA) for albiglutide (Bush et al., 2009; Trujillo and Nuffer, 2014b) or IgG4 Fc fragments for dulaglutide (Jimenez-Solem et al., 2010; Dungan et al., 2016), chemical lipidation for liraglutide (Edgerton et al., 2014; Zaykov et al., 2016), and PEGylation (Kim et al., 2011; Yun et al., 2018).

In this study, we prepared two unclassical structures of exenatide mono-PEGylates and investigated their in-serum stability and hypoglycemic bioactivity. Polyethylene glycol (PEG) was chosen because of its ability to increase the hydrodynamic size to decrease renal filtration and improve anti-proteolysis stability (Lee et al., 2007; Abuchowski et al., 1977; Roberts et al., 2012; Yamaoka et al., 1994). The first unclassical structure of the mono-PEGylate is a branched form ("T-shaped"). Here, a PEG molecule is conjugated to the middle of the exenatide peptide chain, at which lysine residue was point-mutated to cysteine. We investigated the differences inserum stability and hypoglycemic activity between the branched form and the more classical linear form, in which a PEG molecule is conjugated to the C-terminus of

* Corresponding authors.
E-mail addresses: vincero78@hanyang.ac.kr (S.H. Lee), eklee@hanyang.ac.kr (E.K. Lee).
[1] Current address: Biologics Research Center, CKD Pharmaceutics, Ltd., Yongin, Korea.
[2] Immunoforge, Ltd, Seoul, Korea.

https://doi.org/10.1016/j.jbiotec.2019.09.016
Received 24 July 2019; Received in revised form 25 September 2019; Accepted 29 September 2019
Available online 30 September 2019
0168-1656/ © 2019 Published by Elsevier B.V.

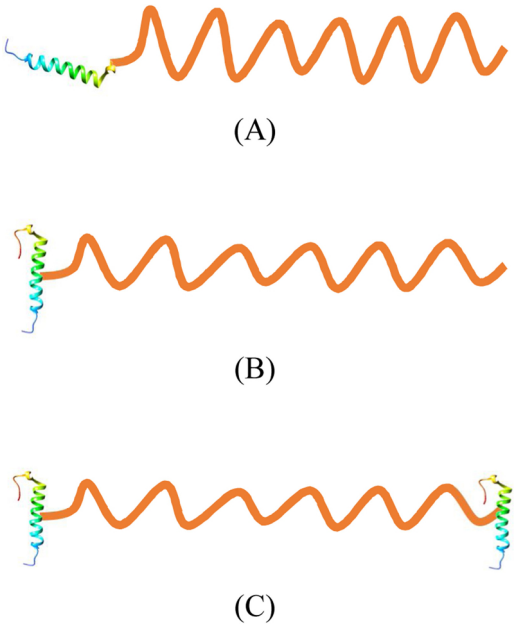

Fig. 1. Configurations of the three types of PEGylates in this study: (A) linear, (B) branched (T-shaped), and (C) homodimer (H-shaped) forms. The helix indicates exenatide and the wavy curve indicates PEG.

the peptide chain (Kim et al., 2012). In addition, we examined the effects of PEG MW on in-serum stability and hypoglycemic activity by conjugating various molecular weights of PEG of the branched form.

The second unclassical structure is a homodimeric mono-PEGylate, in which a bifunctional PEG molecule is conjugated in between the middle of the two identical exenatide mutants for "H-shaped" structure. Our objective was to simultaneously achieve higher potency and improved stability by assembling two exenatide analogs into one PEGylate. We compared *in vitro* and *in vivo* potency and efficacy of this homodimer PEGylate with those of the monomeric PEGylate, using cell-based potency assays and a nude and db/db mouse models.

Fig. 1 depicts the configurations of the three PEGylate studied: the classical linear form, the branched T-shaped form, and the dimeric H-shaped form.

2. Materials and methods

2.1. Materials

Chemically synthesized exenatide (MW 4187 Da) with the following amino acid sequence, HGEGTFTSDLSKQMEEEAVRLFIEWLKNGGPSSG-APPPS-NH_2, was purchased from CS Bio Co. (Menlo Park, CA, USA). Two types of exenatide analogs were prepared by point-mutation; in the first one (K12C) the lysine residue at the 12th position was replaced with cysteine (MW 4162 Da), and in the second one (C40) a cysteine residue was attached to the C-terminus as the 40th residue (4292 Da). The objective of the point-mutation was to achieve residue-specific mono-PEGylation between the thiol group of the peptide and the maleimide group of PEG. The two exenatide analogs were synthesized and purchased from GL Biochem Ltd. (Shanghai, China). PEG maleimide (PEG-MA) and PEG bifunctional maleimide (MA-PEG-MA) were purchased from NOF Corporation (Tokyo, Japan). The buffer and SDS-PAGE chemicals were purchased from Invitrogen Co. (Seoul, Korea). Ion exchange chromatography columns (HiTrap Q® and SP®) were purchased from GE Healthcare (Piscataway, NJ, USA). Flamma® 675 vinylsulfone fluorescence dye was purchased from Bioacts Corporation (Incheon, Korea). Other reagents were purchased from Sigma-Aldrich (St. Louis, MO, USA).

2.2. Preparation of mono- and homodimer PEGylates

Mono-PEGylates of K12C (K12C-PEG) and C40 (C40-PEG) were prepared using a modified procedure described previously (Lee et al., 2007). Briefly, 1 mg/ml of exenatide analog (K12C or C40) was dissolved in 10 mM PBS pH 7.4 containing 5 mM EDTA. The mono-PEGylate was prepared by mixing the analog and PEG-MA at a molar ratio of 1 (exenatide analog) to 1.2 (PEG-MA), or 2 (exenatide analog) to 1 (MA-PEG-MA) for the homodimer PEGylate. The PEGylates were purified by cation exchange chromatography (HiTrap SP, 1 ml) using a BioLogic system (Bio-Rad, Hercules, CA, USA). Ten mM citric acid pH 3.0 was used as Buffer A for the equilibrium buffer. After sample loading, the column was washed with 5 column volumes (CV) of Buffer A. The elution buffer was Buffer A containing 1 M NaCl. A linear gradient from 0% to 40% or 60% for 40 min was applied in the elution step. The flow rate was 1 ml/min and the detection was performed at 280 nm. All experiments were performed at room temperature.

2.3. In vitro bioactivity assay for GLP-1 receptor mediated cMAP secretion

The *in vitro* bioactivity of the PEGylates was measured using a cAMP Hunter Exendin-4 Bioassay kit (Discover X Corp., Fremont, CA, USA). Briefly, engineered CHO cells with GLP-1 receptors expressed on their surfaces were cultured in a 96-well plate at an initial cell density of *ca.* 1.0×10^4 cells/well and incubated in 95% air/5% CO_2 for 24 h. After aspiration, varying concentrations (10^{-7} – 10^{-12} M) of the native exenatide or the PEGylates were added. When exenatide binds to the GLP-1 receptor, the receptor modulates intracellular cAMP production by stimulating adenylate cyclase that is involved in a series of secondary messenger cascades. After incubation, a cell lysis buffer was added to release the intracellular cAMP, and the amount of accumulated cAMP was measured by a luminescence plate reader. The receptor binding bioactivity is determined by the cAMP levels by competitive immunoassay based on enzyme fragment complementation (EFC) technology. A logistic function fitting program (Origin Pro 8) was used to establish a standard curve, from which the amount of cAMP secreted by each PEGylate was determined.

2.4. Sources and handling of experimental animals

All mouse experiments were performed at the Center for Laboratory Animal Science at Hanyang University. The animal protocol was approved by the Institutional Animal Care and Use Committee (IACUC) of Hanyang University (Nos. 2017–0146 and 2017–0233). Nude mice BALB/c (male, 5 weeks old) and Type 2 diabetic BKS.Cg-Dock7^{m}+/+Lepr^{db}/*J* mice (male, 5 or 6 weeks old) were purchased from Orient Bio Co. Ltd. (Seongnam, Korea). The animals were housed in cages in groups of 2 to 3, under a 12 h light/dark cycle (lights off at 8 pm), allowed food and water access, and acclimatized for one week.

2.5. Half-life monitoring of exenatide and PEGylates in nude mice

The native exenatide, the exenatide variants (K12C and C40), and their mono-PEGylates (1 mg/ml) were labeled with a 5 M equivalent of fluorescence dye (Flamma® 675 vinylsulfone, Bioacts Inc., Incheon, Korea) in a 50 mM borate buffer (pH 8.8) at 35 °C overnight in the dark with continuous stirring. Then, the peptide-dye conjugates were purified using a SEC column (PD MiniTrap G-25, GE Healthcare, Uppsala, Sweden) and their buffers were changed to 10 mM PBS buffer (pH 7.4). The concentrations of the peptide-dye conjugates were determined by the dye manufacturer's protocol. Each sample was injected subcutaneously (s.c) into nude mice. At predetermined time points, whole-body fluorescence was measured by an *in vivo* imaging system (Lumina XRMS, PerkinElmer, Akron, OH, USA) at an excitation wavelength of 675 nm and emission wavelength of 691 nm.

2.6. In vivo glucose tolerance test (IPGTT) with db/db mice

The glucose tolerance effects of the native exenatide, the analogs, and the PEGylates were measured in db/db mice. Mice were randomly divided into groups (n = 5). Before sample injection, the mice were fasted overnight. On day 1, one hour prior to the first i.p glucose challenge (0.2 ml, 1.0 g-glucose/kg-body weight) (0 h), mice received s.c injections of the native exenatide and the PEGylates (K12C-PEG5kD, K12C-PEG40 kD, K12C-PEG10 kD-K12C, or C40-PEG40 kD), all at a dose of 25 nmol/kg. The native exenatide was used as a positive control and PBS as a negative control. Before blood glucose measurement, the tail was wiped with ethanol and dried, a tiny scratch was made on the ethanol-washed mouse tail using a disposable lancet, and blood samples were withdrawn using a disposable needle. The first blood drop was wiped out, and subsequent blood drops from each mouse at 0, 0.33, 0.66, 1, 1.5, 2, 2.5, 3 and 4 h were subjected to glucose measurement using a glucometer (Code Free, SD Biosensor, Suwon, Korea). Blood glucose levels were also measured one day before the first injection.

2.7. In vivo hypoglycemic activity measurement in dB/dB mice

The hypoglycemic effects of the native exenatide and the PEGylates were measured in db/db mice. Mice were allowed free access to food and water. Blood glucose levels were measured one day before the first injection. On the day of injection, the mice received single s.c injections of PBS, exenatide, K12C-PEG5kD, K12C-PEG40 kD, K12C-PEG10 kD-K12C, or C40-PEG40 kD at 25 nmol/kg. Blood glucose levels were measured as described above at -1, 0, 0.33, 0.66, 1, 1.5, 2, 2.5, 3, 4, 8, 24, 36, 48, 60, 72, 96, 120, 144, 168, and 192 h. Body weights were recorded daily for 96 h.

2.8. Statistical analysis

All results are expressed as the mean ± standard error of the mean (SEM). One-way analysis of variance (ANOVA) or Student's *t*-test were used for group comparisons. A p value < 0.05 was considered statistically significant. Statistical analyses were performed using Origin Pro 8 (OriginLab Corp.).

3. Results and discussion

3.1. PEGylation for mono- and homodimer PEGylates

The two point-mutants, K12C and C40, were reacted with PEG-MA to obtain the branched form (K12C-PEG) or the linear form (C40-PEG), because both K12C and C40 have only one thiol group and thus PEGylation with PEG-MA would result in residue-specific mono-PEGylate (Nguyen et al., 2016). However, the conjugation of bifunctional MA-PEG-MA with K12C could yield several species. Fig. 2 shows three main peaks in the chromatogram; peak #1 represents the unreacted PEG, peak #2 and #3 represents the mono-PEGylate and the desired homodimer PEGylate, respectively. This elution order supports the previous reports that PEGylated peptides are eluted in the order of multi-, di-, and mono-PEGylates, *i.e.*, the more PEG molecules are attached, the shorter the PEGylate retention time (Kim et al., 2012; Nguyen et al., 2016; Seely and Richey, 2001). It is probably due to the charge shielding effect ('swimming' action) of the PEG molecule that reduces the strength of electrostatic interactions between peptide and functional groups on the cation exchange resin (Thi Nguyen et al., 2018). The molecular weights of peak #2 and peak #3 were determined by MALDI-TOF MS. As shown in Fig. 3, peak #2 was a mixture of the mono-PEGylate (K12C-PEG10 kD; 15,141 Da) and the homodimer PEGylate (19,208 Da), while peak #3 was the homodimer PEGylate (K12C-PEG10 kD-K12C; 19,262 Da). All experimental mass-to-charge (m/z) values closely matched the theoretical calculated values, approximately 14,200 Da for the mono-PEGylate and 18,400 Da for the homodimer PEGylate. The differences in the theoretical and measured MWs (941 Da and 862 Da) seemed to be caused by the polydispersity of the MW distribution of the PEG polymer itself. It was reported that for low MW PEGs (3–5 kD) the polydispersity is ± 1.01, whereas for higher MW PEGs (> 20 kD) it is increased to ± 1.20 (Veronese, 2001). For the 10 kD PEG that we used, it could be ± 1.08-1.09, which explainsthe discrepency between the observed and theoretical MWs.

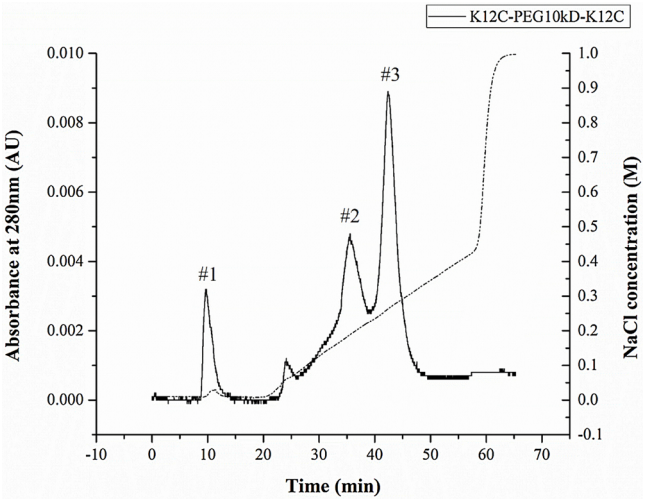

Fig. 2. Cation exchange (HiTrap SP) chromatography separation of homodimeric PEGylate of K12C analogs, K12C-PEG(10 kD)-K12C, from a linear gradient elution from 0 to 400 mM NaCl. Peak #1 represents the unreacted PEG, peak #2 represents the mono-PEGylated K12C (K12C-PEG), and peak #3 represents the homodimer PEGylate (K12C-PEG-K12C).

3.2. In vitro bioactivity assay for GLP-1 receptor mediated cMAP secretion

The effect of the MW of PEG conjugated to K12C on cAMP production in the engineered CHO cells was measured. Fig. 4**(A)** indicates that K12C-PEG40 kD has the highest efficacy of cAMP production compared with the other lower MW PEGylates, but we observed no significant differences in potency values. Table 1 (Expt #1) demonstrates that as PEG MW increases, the potency of the PEGylates appears to decrease, with the exception of PEG 10 kD. However, the trend was not clear enough. It is known that, in general, bioactivity of PEGylates is expected to decrease as PEG MW increases (Lee et al., 2007), probably because longer PEG chains could more effectively mask or shield the activities of the amino acids adjacent to the conjugation site (Thi Nguyen et al., 2018). This phenomenon could hinder the binding between the PEGylates and the receptor, which would result in decreased potency.

Fig. 4**(B)** and Table 1 (Expt #2) demonstrate that the branched K12C-PEG is superior to the linear C40-PEG in both potency and efficacy. A linear PEGylate was expected to increase the affinity to the receptors due to the reduced steric hindrance compared to the branched form (Chae et al., 2007). However, our result as well as other reports indicate the higher MW and branched form PEGs could yield higher bioactivity such as stronger affinity to GLP-1 receptor than the linear form (Kim et al., 2012; Lee et al., 2016; Kim et al., 2010; Fee, 2007). This improved bioactivity of the complexed structures could be in part due to the improved in-serum stability coming from reduced kidney filtration, increased anti-proteolysis, and decreased immunogenicity. It is speculated that PEG conjugation to the C-terminus would induce the shielding (or steric hindrance) effect to not only a number of amino acids near the C-terminus but those near the binding site.

The cAMP production of the branched (T-shaped) mono-PEGylate (K12C-PEG10 kD) was compared to that of the H-shaped homodimer PEGylate (K12C-PEG10 kD-K12C). Fig. 4**(C)** and Table 1 (Expt #3)

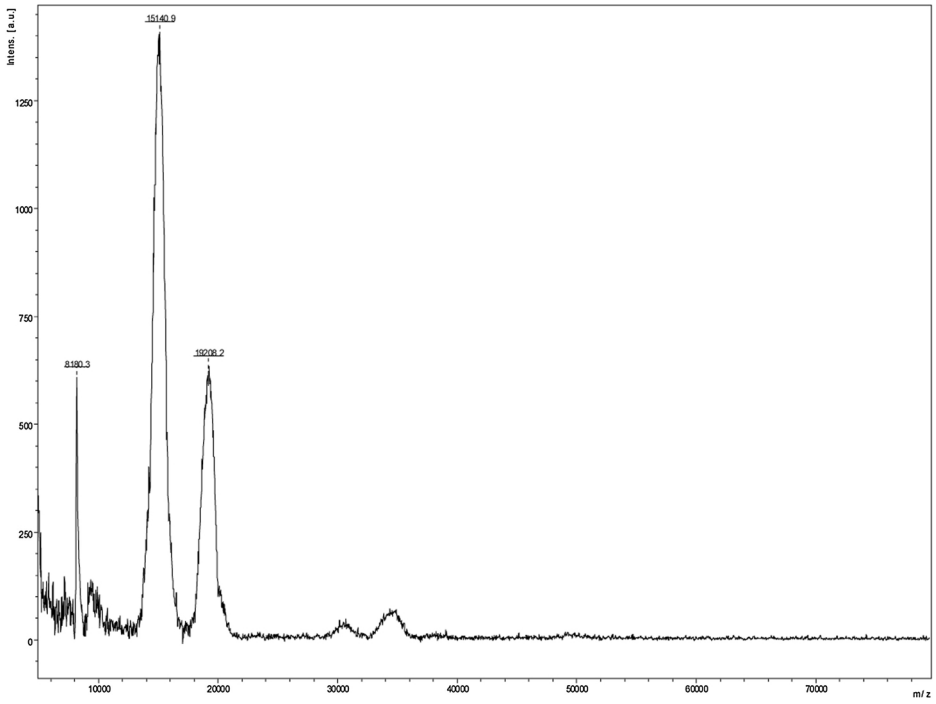

(A)

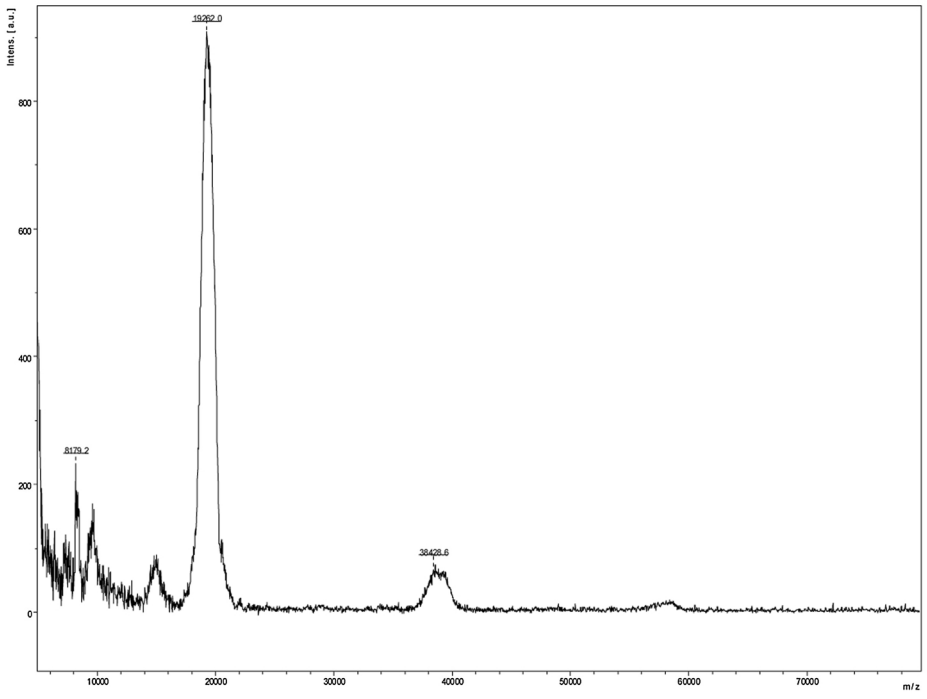

(B)

Fig. 3. MALDI-TOF mass spectra of peak #2 and peak #3 from cation exchange chromatography. (A) Peak #2 represents a mixture between the mono- and homodimer PEGylates (MW 15,141 and 19,208 Da). (B) Peak #3 represents the homodimer PEGylate, K12C-PEG-K12C (MW 19,262 Da).

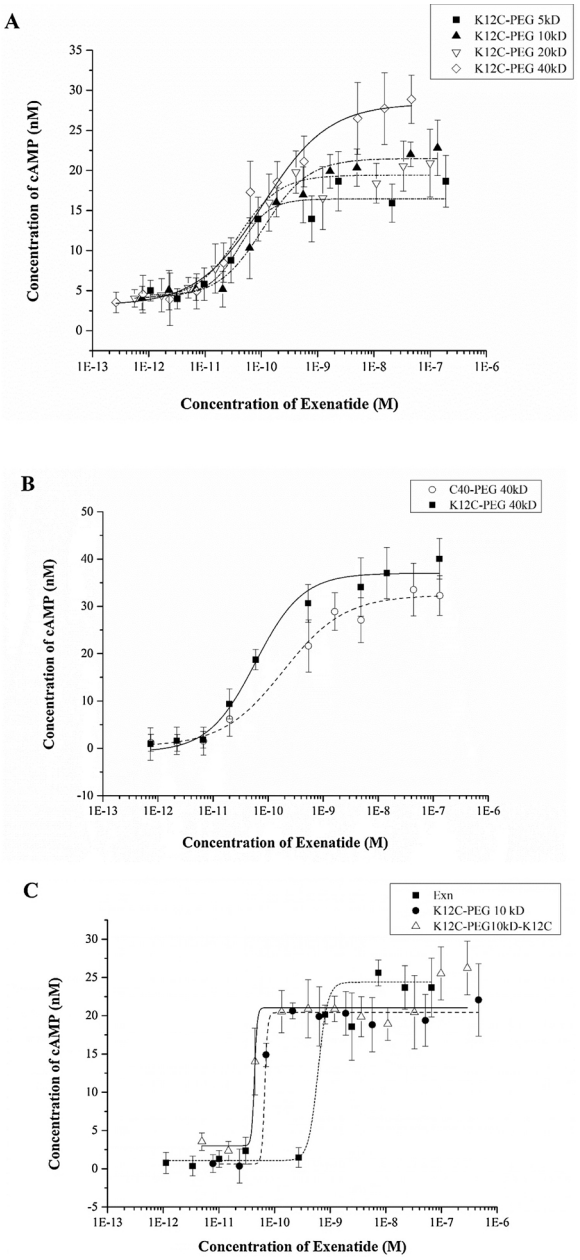

Fig. 4. cAMP production profiles from engineered CHO cells after treatment with: (A) PEGylated K12Cs of various molecular weights (5, 10, 20 and 40 kD), (B) mono-PEGylates of branched form (K12C-PEG 40 KD) and linear form (C40-PEG 40 kD), (C) native exenatide (Exn), mono-PEGylate (K12C-PEG 10 kD), and homodimeric PEGylate (K12C-PEG 10 kD-K12C). Results are plotted as mean ± SEM, n = 3. EC_{50} and E_{max} are summarized in Table 1.

show that the half-maximum effective concentration (EC_{50}) of the homodimer PEGylate was *ca.* 1.5-fold and 14-fold lower than that of the mono-PEGylate (K12C-PEG10 kD) and the native exenatide, respectively. In terms of efficacy, which is an indicator of cAMP production ability, both the monomeric and homodimer PEGylates showed slightly decreased efficacy compared to the native exenatide. Since a dimer may provide a new ligand binding site unlike the single site of a monomer (Aggarwal et al., 2006), use of a dimeric ligand is an alternative approach to improve binding affinity between a ligand and a receptor, and thus potency. The increased potency of the homodimer PEGylate observed in this study could be due to such increased affinity. Overall, the homodimer PEGylate exhibited significantly improved potency compared to the native exenatide, but slightly reduced efficacy.

3.3. Biodistributions of exenatide and PEGylates

The distributions of native exenatide and the PEGylates in nude mice were monitored by non-invasive imaging. Fig. 5**(A)** shows the fluorescence decays of each sample at various time intervals after injection. Strong NIR fluorescence was detected on the backs of the nude mice. To calculate the half-life of each sample, the fluorescence intensity was normalized between the maximum and the minimum values and the fluorescence decay profiles after the single dose administration were fitted using the following first-order elimination equation:

$$C_t = C_0\, e^{-kt}$$

Where C_t is the fluorescent signal intensity after time t, C_0 is the initial fluorescence intensity (t = 0), and k is the elimination rate constant. The relationship between the elimination rate constant and half-life is given by the following equation:

$$t1/2 = \frac{ln2}{k}$$

Fig. 5**(B)** shows the time-course changes of each sample, and Table 2 summarizes their in-serum half-life data. Compared to 1.6 h (native exenatide), both K12C-PEG40 kD and C40-PEG40 kD demonstrated extended half-lives longer than 5 h, while both the native exenatide and K12C-PEG5kD showed similar elimination rates. However, K12C-PEG10 kD-K12C had a relatively short half-life (2.1 h), similar to that of the native peptide. The MW of the homodimer K12C-PEG10 kD-K12C is approximately 19.2 kD, and it could be relatively easily cleared by kidney filtration. This result suggests that molecular size of a PEGylate is critical to its *in vivo* stability.

3.4. In vivo glucose tolerance test (IPGTT)

The ability of each PEGylate to lower blood glucose levels in a mouse model of diabetes was evaluated by IPGTT. As illustrated in Fig. 6, the native exenatide and the exenatide PEGylates remarkably decreased blood glucose levels after glucose challenge; the blood glucose increase for PBS (a negative control) at 1 h after the glucose

Table 1
Comparisons of cAMP producing bioactivities.

Expt #	Objective	Sample	Potency (EC_{50}) (M)	Efficacy (nM cAMP)
1	Effect of PEG MW on cAMP producing bioactivity	K12C-PEG 5 kD	$4.0 \times 10^{-11} \pm 1.4 \times 10^{-12}$	16.4 ± 0.9
		K12C-PEG 10 kD	$1.1 \times 10^{-10} \pm 2.2 \times 10^{-11}$	21.5 ± 0.7
		K12C-PEG 20 kD	$3.8 \times 10^{-11} \pm 1.3 \times 10^{-12}$	19.4 ± 0.7
		K12C-PEG 40 kD	$1.0 \times 10^{-10} \pm 2.9 \times 10^{-11}$	28.3 ± 1.4
2	Comparison of bioactivity between linear form (C40-PEG) and branched form (K12C-PEG) mono-PEGylates.	K12C-PEG 40 kD	$5.9 \times 10^{-11} \pm 1.1 \times 10^{-12}$	37.0 ± 1.8
		C40-PEG 40 kD	$1.9 \times 10^{-10} \pm 7.1 \times 10^{-11}$	32.3 ± 1.5
3	Comparison of bioactivity between native exenatide, mono-PEGylate, and homodimeric PEGylates	Native exenatide	$6.1 \times 10^{-10} \pm 9.3 \times 10^{-11}$	24.4 ± 1.0
		K12C-PEG 10 kD	$6.6 \times 10^{-11} \pm 3.1 \times 10^{-12}$	20.4 ± 0.3
		K12C-PEG 10 kD-K12C	$4.4 \times 10^{-11} \pm 4.9 \times 10^{-12}$	21.1 ± 0.9

Note: EC_{50} and E_{max} values are derived from cAMP response curves in Fig. 4. EC_{50} values are reported as mean ± SEM, n = 3.

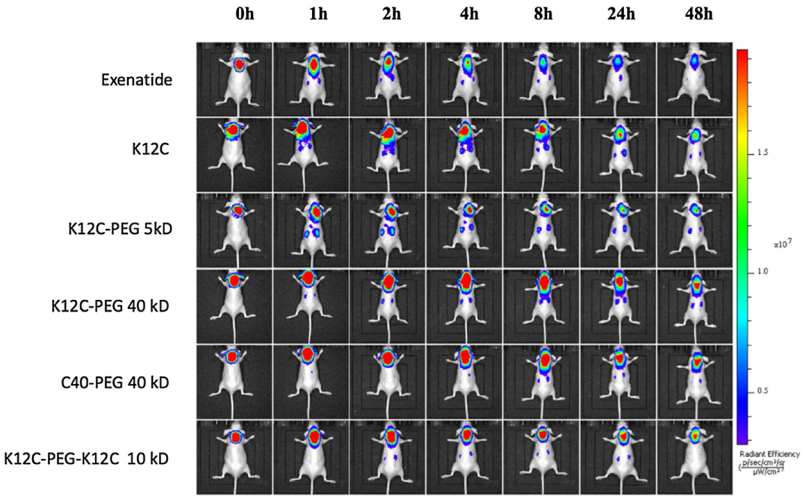

(A)

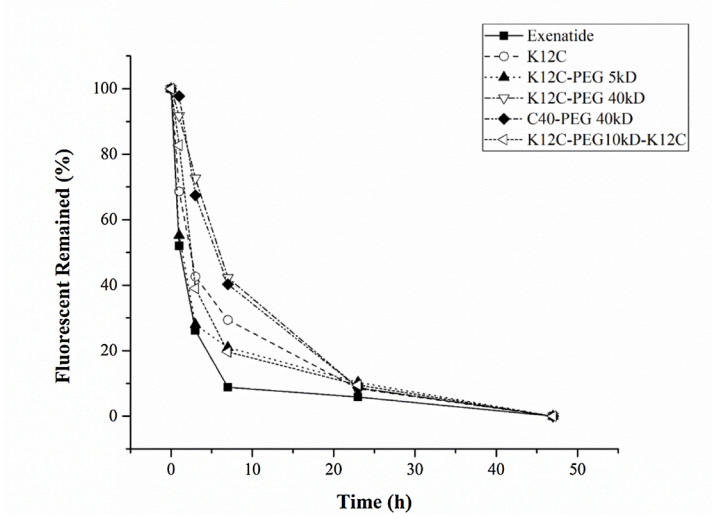

Fig. 5. Fluorescence intensity was monitored in nude mice by non-invasive live imaging at 0, 1, 2, 4, 8, 24, and 48 h after subcutaneous injection of fluorescence-conjugated exenatide, its variant, and various PEGylates.

Table 2
Half-life of each sample calculated from *in vivo* monitoring of fluorescence intensity in nude mice.

Sample	Half-life	R^2
Exenatide	1.6 h	0.969
K12C	2.5 h	0.985
K12C-PEG 5kD	1.7 h	0.977
K12C-PEG 40 kD	5.5 h	0.996
C40-PEG 40 kD	5.1 h	0.986
K12C-PEG 10 kD-K12C	2.1 h	0.980

injection was 260 ± 24 mg/dL, while those for the native exenatide, K12C-PEG5kD, and K12C-PEG10 kD-K12C were 86 ± 38, 69 ± 46, and 172 ± 24 mg/dL, respectively. For K12C-PEG40 kD and C40-PEG40 kD, the amounts of increase were 175 ± 92 and 111 ± 48 mg/dL, respectively. While the AUC of the native exenatide (2480) was not much different from that of PBS (2798), all PEGylates showed significantly reduced AUCs compared to the native exenatide. These findings indicate that PEGylates have stronger glucose-lowering activity *in vivo* compared to native exenatide. The AUCs of K12C-PEG5kD (2133) and K12C-PEG10 kD-K12C (2233) were significantly lower than that of the PBS control ($p < 0.05$). Both the branched and the linear forms of PEGylates at the same MW (K12C-PEG40 kD and C40-PEG40 kD) showed very similar AUCs; 2467 and 2,494, respectively. Interestingly, K12C-PEG5kD and the homodimer (K12C-PEG10 kD-K12C) decreased blood glucose levels immediately after glucose challenge at 0 h, a different trend from that seen in other samples.

3.5. *In vivo* hypoglycemic activity and its duration

We studied the long-term hypoglycemic effects in a mouse model of diabetes. Mice were allowed free access to food and water, and blood glucose levels were monitored for up to 192 h after sample injection until they reached the baseline. As shown in Fig. 7, the blood glucose level of the negative control group (PBS) remained constant at approximately 600 mg/dL. The native exenatide decreased glucose levels for about 90 min, and then the level started to increase after 2 h and reached the control baseline after about 12 h. For K12C-PEG5kD, the level came to baseline after about 60 h. Both the linear C40-PEG40 kD and the branched K12C-PEG40 kD allowed the level to reach the baseline after nearly 130 h and 140 h, respectively. In particular, the time required for the homodimer PEGylate (K12C-PEG10 kD-K12C) to reach the baseline was approximately 168 h. This demonstrated that the

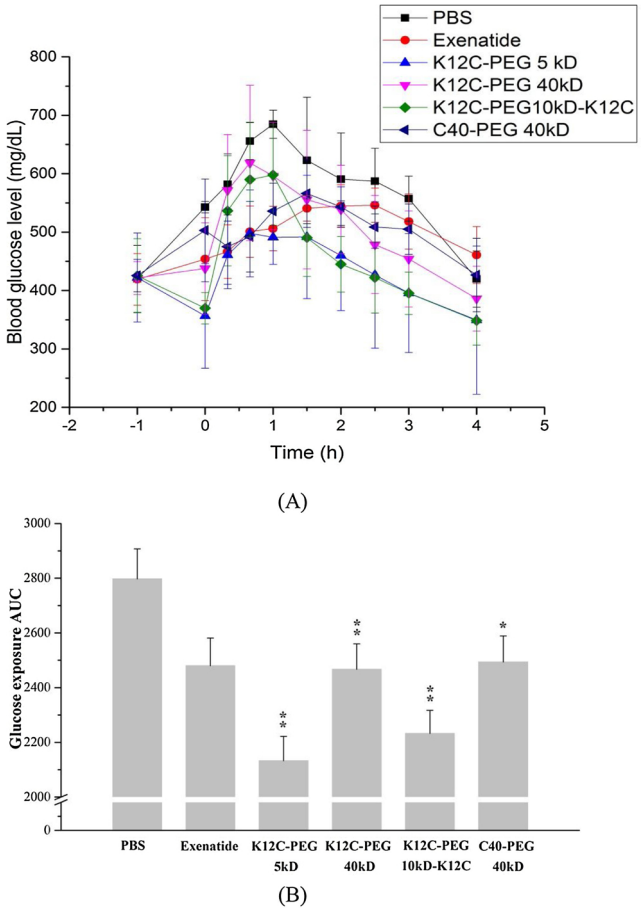

Fig. 6. IPGTT results for exenatide and various PEGylates in diabetic mice. Mouse blood glucose levels were measured after a single subcutaneous injection of exenatide and the samples were maintained at 25 nmol/kg. After 1 h, glucose was intraperitoneally injected at 1.0 g/kg at time 0 h. All data were compared to mice injected with PBS (negative control) of an equivalent volume. Values are expressed as mean ± SEM, n = 5 (in B, C, D, E) or n = 3 (in A). AUCs were compared using two-tailed *t*-test (*p < 0.05, **p < 0.01).

branched and the homodimer PEGylates extended the time approximately 12- and 14-fold, respectively, compared to the native exenatide. It should be noted that only one small dose (25 nmol kg^{-1}) of K12C-PEG40 kD and the homodimer PEGylate (K12C-PEG10 kD-K12C) extended the time similar to that of the dose, 150 or 250 nmol·kg^{-1}, used in other studies (Han et al., 2017; Pan et al., 2006). This result also suggests that PEG MW plays a key role in extending the duration of hypoglycemic activity: the higher the PEG MW, the longer the duration, probably due to the increased shielding effect of PEG (Thi Nguyen et al., 2018; Lee and Lee, 2017).

On the other hand, the homodimer PEGylate (K12C-PEG10 kD-K12C) demonstrated much stronger hypoglycemic activity, especially during the initial period (up to 36 h), probably because of the increased potency of the dimer. The MW of the PEGylate is approximately 19.2 kD, much lower than that of K12C-PEG40 kD (*ca.* 44.2 kD), but is more effective for extending the hypoglycemic state to approximately 30 h. This effect may be attributed to the H-shaped molecular structure, which would strengthen the receptor binding to render higher potency, despite the relatively shorter *in vivo* half-life observed earlier.

4. Conclusions

Our findings highlight the exenatide PEGylates in unclassical structures, other than the classical linear structure, can extend hypoglycemic activity and improve stability. PEG MW appears to play an important role for in-serum stability and hypoglycemic activity. The branched configuration shows superior *in vitro* receptor binding and *in vivo* hypoglycemic activity than the linear counterpart. Compared to the native peptide, these unclassical structures of the T-shaped branched and the H-shaped homodimer form not only improved the *in vivo* potency by more than 10-fold but also extended glucose-lowering activity by more than 12-fold. In sum, the PEGylates of the unclassical structures appear to be promising candidates for next-generation long-acting peptide drugs. Further investigation is warranted to determine the modes of action underlying their potency and stability.

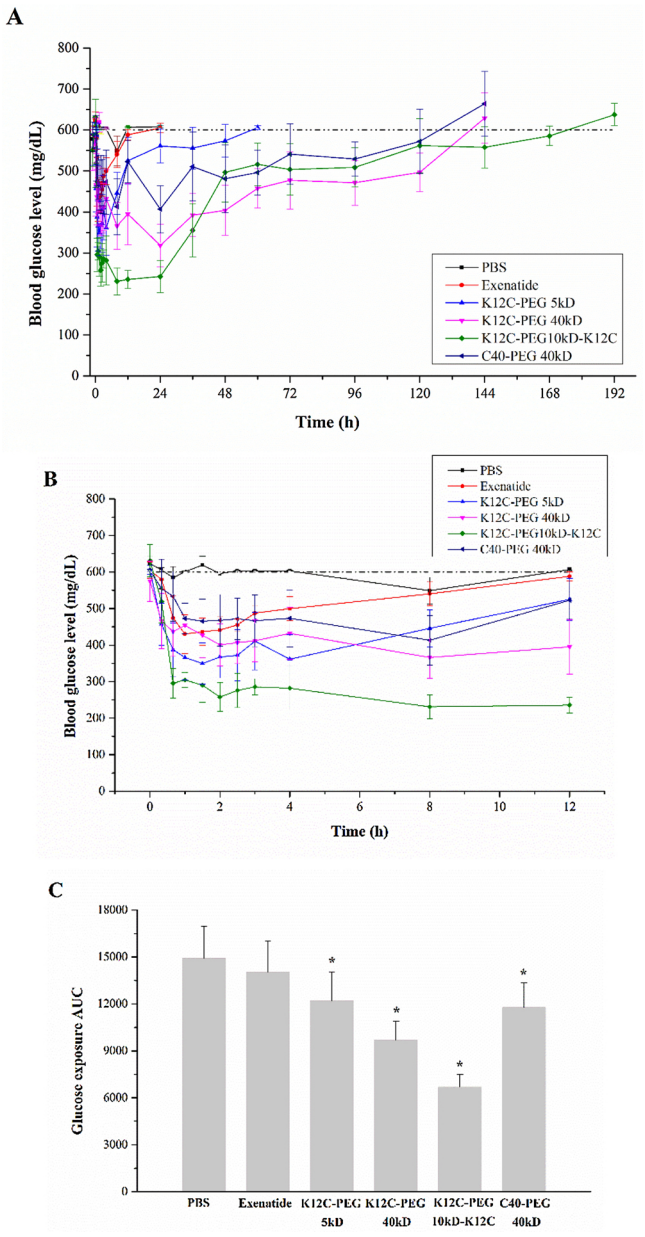

Fig. 7. Hypoglycemic duration of exenatide and the various PEGylates in db/db mice for: (A) up to 192 h, and (B) up to 12 h. Mouse blood glucose levels were measured after single subcutaneous injection of exenatide and the samples at 25 nmol/kg and PBS of an equivalent volume. (C) Hypoglycemic values are expressed as a mean ± SEM; n = 5 for the sample groups and n = 3 for the control group. AUCs were compared using two-tailed *t*-test, *p < 0.05.

Declaration of Competing Interest

The authors declare that they have no known competing financial

interests or personal relationships that could have appeared to influence the work reported in this paper.

Acknowledgments

This work was supported by a National Research Foundation (NRF) of Korea grant funded by the Korean government (MSIP) (No.2014R1A2A2A03004266).

References

Lund, A., Knop, F.K., Vilsbøll, T., 2014. Glucagon-like peptide-1 receptor agonists for the treatment of type 2 diabetes: differences and similarities. Eur. J. Intern. Med. 25, 407–414.

Trujillo, J.M., Nuffer, W., 2014a. GLP-1 receptor agonists for type 2 diabetes mellitus: recent developments and emerging agents. Pharmacother.: J. Hum. Pharmacol. Drug Ther. 34, 1174–1186.

Edwards, C.M.B., Stanley, S.A., Davis, R., Brynes, A.E., Frost, G.S., Seal, L.J., Ghatei, M.A., Bloom, S.R., 2001. Exendin-4 reduces fasting and postprandial glucose and decreases energy intake in healthy volunteers. Am. J. Physiol.-Endocrinol. Metabol. 281, E155–E161.

Egan, J.M., Clocquet, A.R., Elahi, D., 2002. The insulinotropic effect of acute exendin-4 administered to humans: comparison of nondiabetic state to type 2 diabetes. J. Clin. Endocrinol. Metab. 87, 1282–1290.

Gentilella, R., Bianchi, C., Rossi, A., Rotella, C., 2009. Exenatide: a review from pharmacology to clinical practice. Diabetes Obes. Metab. 11, 544–556.

Bush, M., Matthews, J., De Boever, E., Dobbins, R., Hodge, R., Walker, S., Holland, M., Gutierrez, M., Stewart, M., 2009. Safety, tolerability, pharmacodynamics and pharmacokinetics of albiglutide, a long-acting glucagon-like peptide-1 mimetic, in healthy subjects. Diabetes Obes. Metab. 11, 498–505.

Trujillo, J.M., Nuffer, W., 2014b. Albiglutide: a new GLP-1 receptor agonist for the treatment of type 2 diabetes. Ann. Pharmacother. 48, 1494–1501.

Jimenez-Solem, E., Rasmussen, M.H., Christensen, M., Knop, F.K., 2010. Dulaglutide, a long-acting GLP-1 analog fused with an Fc antibody fragment for the potential treatment of type 2 diabetes. Curr. Opin. Mol. Ther. 12, 790–797.

Dungan, K., Raz, I., Skrivanek, Z., Sealls, W., Fahrbach, J., 2016. Achieving the composite endpoint of glycated haemoglobin < 7.0%, no weight gain and no hypoglycaemia in the once-weekly dulaglutide AWARD programme. Diabetes Obes. Metab. 18, 49–55.

Edgerton, D.S., Moore, M.C., Winnick, J.J., Scott, M., Farmer, B., Naver, H., Jeppesen, C.B., Madsen, P., Kjeldsen, T.B., Nishimura, E., 2014. Changes in glucose and fat metabolism in response to the administration of a hepato-preferential insulin analog. Diabetes 63, 3946–3954.

Zaykov, A.N., Mayer, J.P., DiMarchi, R.D., 2016. Pursuit of a perfect insulin. Nat. Rev. Drug Discov. 15, 425–439.

Kim, T.H., Jiang, H.H., Lee, S., Youn, Y.S., Park, C.W., Byun, Y., Chen, X., Lee, K.C., 2011. Mono-PEGylated dimeric exendin-4 as high receptor binding and long-acting conjugates for type 2 anti-diabetes therapeutics. Bioconjug. Chem. 22, 625–632.

Yun, S.P., Kam, T.-I., Panicker, N., Kim, S., Oh, Y., Park, J.-S., Kwon, S.-H., Park, Y.J., Karuppagounder, S.S., Park, H., 2018. Block of A1 astrocyte conversion by microglia is neuroprotective in models of Parkinson's disease. Nat. Med. 24, 931–938.

Lee, B.K., Kwon, J.S., Kim, H.J., Yamamoto, S., Lee, E., 2007. Solid-phase PEGylation of recombinant interferon α-2a for site-specific modification: process performance, characterization, and in vitro bioactivity. Bioconjug. Chem. 18, 1728–1734.

Abuchowski, A., McCoy, J.R., Palczuk, N.C., van Es, T., Davis, F.F., 1977. Effect of covalent attachment of polyethylene glycol on immunogenicity and circulating life of bovine liver catalase. J. Biol. Chem. 252, 3582–3586.

Roberts, M., Bentley, M., Harris, J., 2012. Chemistry for peptide and protein PEGylation. Adv. Drug Deliv. Rev. 64, 116–127.

Yamaoka, T., Tabata, Y., Ikada, Y., 1994. Distribution and tissue uptake of poly (ethylene glycol) with different molecular weights after intravenous administration to mice. J. Pharm. Sci. 83, 601–606.

Kim, T.H., Jiang, H.H., Lim, S.M., Youn, Y.S., Choi, K.Y., Lee, S., Chen, X., Byun, Y., Lee, K.C., 2012. Site-specific PEGylated Exendin-4 modified with a high molecular weight trimeric PEG reduces steric hindrance and increases type 2 antidiabetic therapeutic effects. Bioconjug. Chem. 23, 2214–2220.

Nguyen, N.-T.T., Lee, J.S., Yun, S., Lee, E., 2016. Separation of mono-and di-PEGylate of exenatide and resolution of positional isomers of mono-PEGylates by preparative ion exchange chromatography. J. Chromatogr. A 1457, 88–96.

Seely, J.E., Richey, C.W., 2001. Use of ion-exchange chromatography and hydrophobic interaction chromatography in the preparation and recovery of polyethylene glycol-linked proteins. J. Chromatogr. A 908, 235–241.

Thi Nguyen, N.-T., Yun, S., Lim, D.W., Lee, E., 2018. Shielding effect of a PEG molecule of a mono-PEGylated peptide varies with PEG chain length. Prep. Biochem. Biotechnol. 48, 522–527.

Veronese, F.M., 2001. Peptide and protein PEGylation: a review of problems and solutions. Biomaterials 22, 405–417.

Chae, S.Y., Jin, C.-H., Shin, H.J., Youn, Y.S., Lee, S., Lee, K.C., 2007. Preparation, characterization, and application of biotinylated and biotin− pegylated glucagon-like peptide-1 analogues for enhanced oral delivery. Bioconjug. Chem. 19, 334–341.

Lee, W., Park, E.J., Kwak, S., Lee, K.C., Na, D.H., Bae, J.-S., 2016. Trimeric peg-conjugated exendin-4 for the treatment of sepsis. Biomacromolecules 17, 1160–1169.

Kim, I., Kim, T.H., Ma, K., Lee, E.S., Kim, D., Oh, K.T., Lee, D.H., Lee, K.C., Youn, Y.S., 2010. Synthesis and evaluation of human serum albumin-modified exendin-4 conjugate via heterobifunctional polyethylene glycol linkage with protracted hypoglycemic efficacy. Bioconjug. Chem. 21, 1513–1519.

Fee, C.J., 2007. Size comparison between proteins PEGylated with branched and linear poly (ethylene glycol) molecules. Biotechnol. Bioeng. 98, 725–731.

Aggarwal, S., Singh, P., Topaloglu, O., Isaacs, J.T., Denmeade, S.R., 2006. A dimeric peptide that binds selectively to prostate-specific membrane antigen and inhibits its enzymatic activity. Cancer Res. 66, 9171–9177.

Han, J., Wang, Y., Meng, Q., Li, G., Huang, F., Wu, S., Fei, Y., Zhou, F., Fu, J., 2017. Design, synthesis and biological evaluation of PEGylated Xenopus glucagon-like peptide-1 derivatives as long-acting hypoglycemic agents. Eur. J. Med. Chem. 132, 81–89.

Pan, C.Q., Buxton, J.M., Yung, S.L., Tom, I., Yang, L., Chen, H., MacDougall, M., Bell, A., Claus, T.H., Clairmont, K.B., 2006. Design of a long acting peptide functioning as both a glucagon-like peptide-1 receptor agonist and a glucagon receptor antagonist. J. Biol. Chem. 281, 12506–12515.

Lee, S., Lee, D.Y., 2017. Glucagon-like peptide-1 and glucagon-like peptide-1 receptor agonists in the treatment of type 2 diabetes. Ann. Pediatr. Endocrinol. Metab. 22, 15–26.